

Nanoparticulate Tungsten Oxide for Catalytic Epoxidations

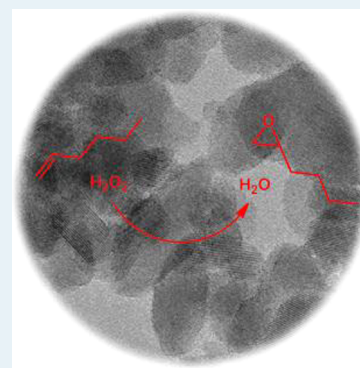
Ceri Hammond,[†] Julian Straus,[†] Marco Righettoni,[‡] Sotiris E. Pratsinis,[‡] and Ive Hermans^{*,†}

[†]Dept. of Chemistry and Applied Biosciences, ETH Zürich, Wolfgang-Pauli-Strasse 10, 8093 Zürich, Switzerland

[‡]Particle Technology Laboratory, Department of Mechanical and Process Engineering, ETH Zürich, 8092 Zürich, Switzerland

Supporting Information

ABSTRACT: A combination of spectroscopic and catalytic investigations led to the surprising conclusion that not isolated W^{VI} species but WO_3 oxide is the most active and stable phase for olefin epoxidation with H_2O_2 . Optimal activity was subsequently found for a nanoparticulate WO_3 prepared by flame aerosol technology. This material is characterized by a 50% increase in activity per W^{VI} site, and a 35-fold increase in space time yield, compared with the current benchmark catalyst.



KEYWORDS: epoxidation. Lewis acid catalysis. sustainable chemistry. flame spray pyrolysis

INTRODUCTION

Epoxides are versatile intermediates that are used throughout the chemical value chain. Ethylene oxide (21 Mt/year) and propylene oxide (9 Mt/year) are, based on scale, the most important examples used in the production of various polymers;¹ however, many other epoxides are used industrially as the starting compound for the synthesis of commodity and specialty chemicals. Epoxides are almost exclusively produced via the oxygenation of an olefin double bond. Although molecular oxygen is the most desirable oxidant from a green and economic viewpoint, to date, its use as a mono-oxygen donor for epoxidation has been successfully demonstrated only for ethylene.¹ As such, the epoxidation of alternative olefins requires more selective mono-oxygen donors, among which percarboxylic acids or alkyl hydroperoxides are the most commonly utilized. Nevertheless, their usage is accompanied by the generation of an equivalent amount of organic byproduct (carboxylic acid or alcohol), thus decreasing atom efficiency and resulting in the generation of large amounts of waste.² The development of greener and more sustainable epoxidation processes is thus an urgent task, and in this regard, the utilization of hydrogen peroxide (H_2O_2) as the oxygen donor is highly favored. Its high active oxygen content and the nontoxic nature of its byproduct (H_2O) are the two major reasons for this.

The key to an efficient epoxidation catalyst is the presence of a Lewis acidic center, which is responsible for activation of the peroxide. Some notable Lewis acids are d^0 metals, such as Ti^{IV} , Mo^{VI} , and W^{VI} , many of which have successfully been applied for decades as homogeneous epoxidation catalysts. A pertinent example is the Venturello–Ishii catalytic system,^{3,4} which combines tungstic acid (H_2WO_4), phosphate species, and

various ammonium and phosphonium counterions to facilitate the selective epoxidation of olefins under three-phase reaction conditions. Nonetheless, although this and other related homogeneous systems are highly active and selective, heterogeneous catalysts are typically preferred on an industrial scale for a number of downstream processing considerations.⁵

Much effort has therefore been devoted to the design and synthesis of equally active and stable heterogeneous analogues. In fact, tremendous success has been achieved in the synthesis of heterogeneous Ti^{IV} -based catalysts. A notable example is the case of propylene oxide production, in which the use of a Ti^{IV} -containing MFI-type zeolite (TS-1) has resulted in a more sustainable epoxidation process, with H_2O_2 as the terminal oxidant.^{5,6} Despite its success, however, the immobilization of Ti^{IV} into the relatively narrow MFI pores results in only propylene being successfully epoxidized. Furthermore, although alternative Ti^{IV} -containing zeolites with larger pores, such as Ti- β and Ti-MWW,^{7,8} overcome this limitation, their activity and selectivity are typically much lower, and their synthesis is fraught with complications. As such, the development of alternative heterogeneous catalysts that are both more generally applicable and easier to synthesize is a challenge of high practical relevance.

Although W^{VI} -based complexes account for some of the most active homogeneous catalysts for H_2O_2 -mediated oxidations,^{3,4,9} attempts to design heterogeneous analogues with sufficient stability and activity have, to date, proven rather unsuccessful. Typical approaches involve the immobilization of

Received: December 18, 2012

Revised: January 18, 2013

Published: January 21, 2013

highly active peroxotungstate complexes into or onto inorganic supports, such as silica-based matrixes or anion-exchange resins.^{10–12} However, the weak interaction between the complex and the support typically leads to some leaching or deactivation of the catalyst, and the immobilization of the homogeneous complex typically leads to poor accessibility and a significant decrease in relative activity.¹³ Another serious limitation arises from residual functionalities in the support material, with basic and hydrophilic sites leading to poor H₂O₂-efficiency. Furthermore, many heterogeneous W^{VI}-based catalysts have been found to be poorly active in the absence of other (co)-catalytic species, such as the bicarbonate anion.¹⁴ As in many cases of heterogeneously catalyzed reactions, the identity and nature of the true active sites and species has also not yet been fully elucidated.

Recently, it was reported that a material prepared by the impregnation of Zn and W to SnO₂ set a new benchmark for H₂O₂-mediated epoxidations.¹⁵ Along with proceeding at high levels of activity and selectivity, the catalyst was found to be generally applicable for a number of olefin substrates, including bulky molecules, such as cyclooctene and cyclododecene. These exciting results prompted us to reevaluate the viability of heterogeneous tungsten-based epoxidation catalysts. In this work, we demonstrate that through a combination of spectroscopic and catalytic studies, a significantly more stable and active material, in terms of both activity per site (i.e., TON/TOF) and space time yield, can be designed for the epoxidation of olefins.

RESULTS AND DISCUSSION

Reproduction of Reported Catalyst. Toward our goal of synthesizing an active and stable tungsten-based, heterogeneous Lewis acid catalyst, we first aimed to reproduce the reported activity of the recently published W–Zn/SnO₂ catalyst to obtain the benchmark catalyst from the literature from which to optimize further. As described by Kamata et al., the preparation of this catalyst proceeds in two steps; first, the additive (Zn) is loaded onto the support and calcined at high temperature (300 °C, 2 h).¹⁵ Subsequently, the Lewis acid (W) is impregnated onto the modified support (Zn/SnO₂), with a second calcination step (400 °C, 3 h), yielding the final catalyst. The kinetic activity of the so-formed catalyst was evaluated through the epoxidation of 1-hexene under conditions identical to those reported by Kamata et al. As can be seen (Table 1), the epoxidation proceeds well over the synthesized catalyst, with a high degree of reproducibility.

Although the observed efficiency of the catalyst is marginally lower than reported, from the comparable epoxide yield and TOF, we conclude that the catalyst has, indeed, been successfully reproduced. Nevertheless, to evaluate this further,

Table 1. Reproduction of Reported Literature Catalyst for the Selective Epoxidation of 1-Hexene^a

entry	H ₂ O ₂ conv (%) ^b	epoxide yield (%) ^c	TOF (h ⁻¹) ^d	ref
1	96	18.2	6.9	15
2	>98	15.9	6.0	this work

^a0.2 M in dimethyl carbonate, DMC. ^bMoles H₂O₂ consumed/initial moles H₂O₂ × 100. ^cMoles epoxide formed/initial moles alkene × 100. ^dMole (epoxide formed) mole⁻¹ (W) h⁻¹. Reaction conditions: 1-hexene in dimethyl carbonate (0.2 M), olefin/H₂O₂ molar ratio = 5.0, 80 °C, 4 h, 3.3 mol % W.

the epoxidation of cyclooctene was also studied; however, under the conditions employed by the authors (H₂O₂/olefin molar ratio 1:1),¹⁵ a triphasic reaction solution was obtained. This third aqueous phase resulted in the coating of the glass reactor with the catalyst, inhibiting dispersion and leading to negligible levels of catalytic activity.

Given the poor suitability of DMC as a solvent, we subsequently evaluated other solvents also reported by the authors. A suitable compromise in terms of solubility of substrate and H₂O₂, catalyst dispersion and activity was obtained with 1-butanol, although the reported yields in this solvent are around 50% lower than for DMC. Nevertheless, under otherwise identical reaction conditions, it can be seen that the epoxidation proceeds smoothly (Figure 1, curve a), with the expected levels of yield and selectivity obtained.

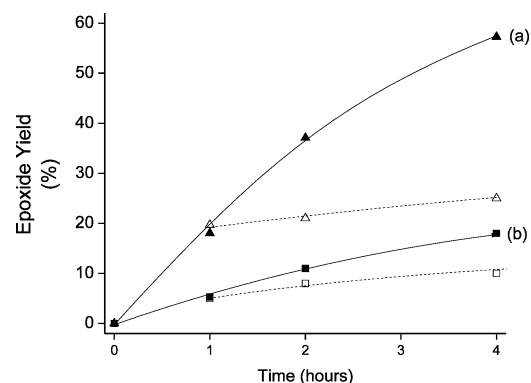


Figure 1. Temporal evolution of cyclooctene oxide under the influence of calcined (a) and uncalcined (b) 3.5 wt % W–0.8 wt % Zn/SnO₂ (reaction in 1-butanol). Open shapes represent the activity of the solution after removal of the solid catalyst. Reaction conditions: cyclooctene in 1-butanol (1.0 M), olefin/H₂O₂ molar ratio = 1.0, 80 °C, 4 h, 0.15 mol % W.

It was previously reported that isolated mono- or polytungstate species were the active sites in the calcined catalysts. This hypothesis was based upon the correlation of catalytic activity with Raman features between 1000 and 900 cm⁻¹, typically observed in mono- and polytungstate species, such as sodium metatungstate and tungstic acid.¹⁵ However, such dioxo groups are absent in the calcined analogue (Figure 2), which is, however, catalytically more active (Figure 1). The Raman signal of the calcined sample is instead dominated by features associated with (bulk) WO₃.²³ Given that the calcined

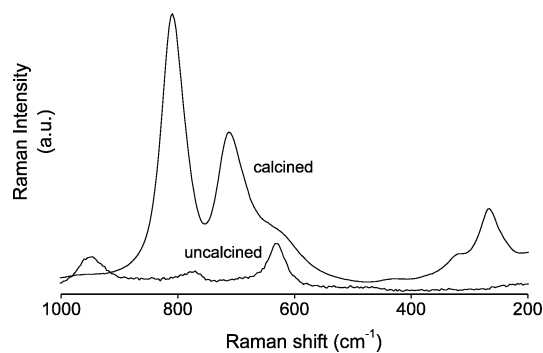


Figure 2. Raman spectra of the 3.5 wt % W–0.8 wt % Zn/SnO₂(IMP) catalyst, before and after calcination.

material is significantly more active than the uncalcined analogue, it is clear that the assignment of mono- and polytungstate species as the active site requires further investigation. The need for investigation is heightened by the observations of Hoegerts et al., who also noted that mono- and ditungstate species, anionically exchanged onto inorganic supports, possess only limited activity and stability during the epoxidation of various olefins, such as cyclooctene.¹¹

Nature of the Active Species. From our initial catalytic and spectroscopic studies, it appears that (bulk) WO_3 is the active phase, as opposed to the mono- or polytungstate species proposed previously. This appears to be highly unusual, since bulk metal oxides are typically thought to be rather undesirable for Lewis acid-mediated transformations, such as H_2O_2 -based epoxidation reactions. Typically, site-isolated (i.e. well-dispersed) Lewis acid centers are thought to be responsible for catalytic activity in such cases. For example, the epoxidation of olefins with H_2O_2 is typically catalyzed by Ti^{IV} species, isolated within inorganic matrixes, such as zeolites (e.g., TS-1).^{5,17} The activation of carbonyl groups by, for example, Sn^{IV} , is also observed over isolated active sites.¹⁸ The isolation of the Lewis acid center leads to an increase in coordinative unsaturation and increases the reactivity of these sites. The immobilization into/onto an inorganic matrix is also believed to increase the coordinative strain on the Lewis acid centers and thereby facilitates the coordination of reacting molecules. As such, the observation that stable, bulk WO_3 species are able to catalyze this reaction is highly significant and surprising.

To test this surprising hypothesis further, the catalytic activity of grained mixtures of WO_3 and SnO_2 were evaluated and compared with impregnated analogues. For these investigations, we note that Zn has been omitted from these materials to simplify evaluation of the active sites. Indeed, Zn has been shown to be a noncatalytic promoter of the catalyst.¹⁵ The role of Zn, with regard to activity and stability, is discussed in depth later.

It is clear from Figure 3 that grinding bulk WO_3 together with SnO_2 (denoted $\text{WO}_3/\text{SnO}_2(\text{PM})$) leads to the formation of a highly active catalyst, comparable in terms of activity and selectivity (>95%) to the impregnated (monometallic) analogue. In fact, at longer reaction times (>2 h), it appears

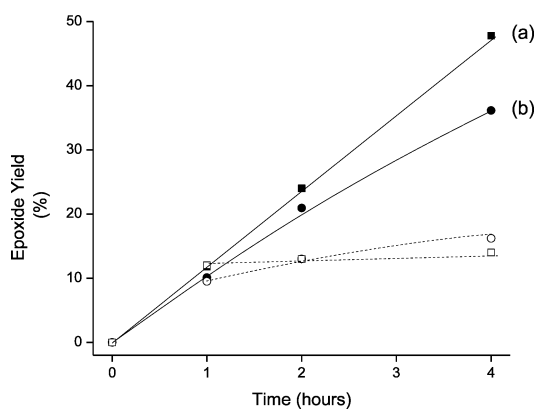


Figure 3. Evolution of cyclooctene oxide under the influence of $\text{WO}_3/\text{SnO}_2(\text{PM})$ (a) and calcined $\text{W}/\text{SnO}_2(\text{IMP})$ (b). The performance of the supernatant obtained in a hot-separation test after 1 h is represented by the corresponding open symbols. Reaction conditions: cyclooctene in 1-butanol (1.0 M), olefin/ H_2O_2 molar ratio = 1.0, 80 °C, 4 h, 0.15 mol % W.

that the mechanically mixed material is, in fact, more active than the impregnated analogue. This is an important observation, since it again indicates that bulk WO_3 species are stable under the reaction conditions, in good agreement with the negative hot-separation test of calcined $\text{W}-\text{Zn}/\text{SnO}_2(\text{IMP})$ (Figure 1), in which WO_3 was the only species detected by Raman spectroscopy. In addition, an excellent linear correlation was found against the amount of WO_3 mixed with SnO_2 and the catalytic activity at a given mass charge of catalyst (Figure 4). As expected, the corresponding Raman signals (Figure 4, inset) are indicative of only bulk WO_3 species, which further strengthens the hypothesis of highly active bulk WO_3 .

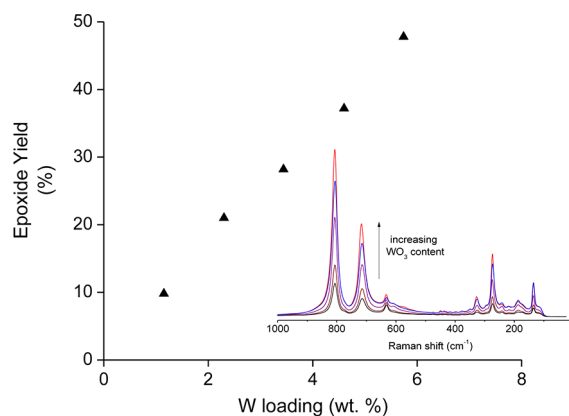


Figure 4. Catalytic activity of $\text{WO}_3/\text{SnO}_2(\text{PM})$ as a function of the W loading. The Raman spectrum of each sample is overlaid as an inset. Reaction conditions: cyclooctene in 1-butanol (1.0 M), olefin/ H_2O_2 molar ratio = 1.0, 80 °C, 4 h, 40 mg catalyst.

Stability of the Active Sites. It was previously proposed that along with being significantly more active, bulk WO_3 appeared to be a more stable catalyst than mono- or polytungstate species. This was based on the rather poor performance of uncalcined $\text{W}-\text{Zn}/\text{SnO}_2(\text{IMP})$ catalyst in the hot-separation test in comparison with the calcined analogue. The epoxide yield obtained with the uncalcined material, containing predominantly mono- and polytungstate species, was found to double, even after removal of the solid catalyst. This indicates a significant amount of leaching and the formation of a highly active homogeneous phase during the reaction, thus suggesting that the uncalcined, impregnated catalyst possesses poor stability. In contrast, after removal of calcined $\text{W}-\text{Zn}/\text{SnO}_2(\text{IMP})$, containing predominately WO_3 , only negligible changes in epoxide yield were observed.

To substantiate this hypothesis further, we investigated the catalytic activity and heterogeneity of unsupported tungstic acid, H_2WO_4 , the W^{VI} precursor used for preparation of the impregnated catalyst, against bulk WO_3 powder. As can be seen (Figure 5), H_2WO_4 appears to be an outstanding catalyst: although producing an excellent epoxide yield, the observed activity is almost exclusively due to the presence of leached metal. In contrast, although unsupported (bulk) WO_3 is less active, presumably because of a low dispersion following removal of the support material, the activity is predominately heterogeneous. These results add weight to the belief that the active, *heterogeneous* epoxidation phase is WO_3 and that mono- and polytungstate species are much more prone to leaching and homogeneous catalysis.

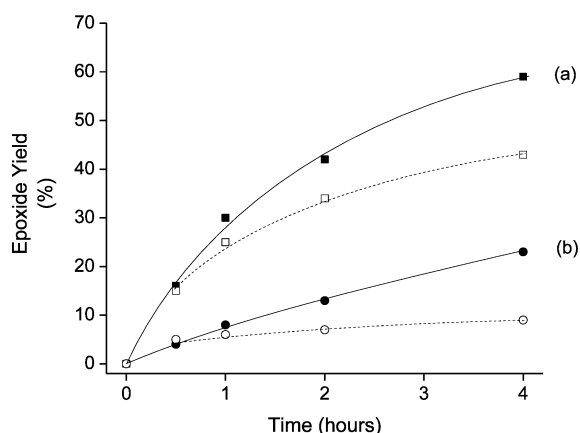


Figure 5. Evolution of cyclooctene oxide under the influence of H_2WO_4 (a) and unsupported WO_3 (b). Open shapes represent the activity of the solution after removal of the catalyst after 0.5 h. Reaction conditions: cyclooctene in 1-butanol (1.0 M), olefin/ H_2O_2 molar ratio = 1.0, 80 °C, 4 h, 0.15 mol % W.

Further confirmation of this hypotheses was obtained by performing hot-separation studies on calcined $\text{W}/\text{SnO}_2(\text{IMP})$ and $\text{WO}_3/\text{SnO}_2(\text{PM})$ catalytic systems (Figure 3). The negative hot-separation test for $\text{WO}_3/\text{SnO}_2(\text{PM})$ confirms that when tungsten is present as bulk oxide, negligible levels of leaching are observed. In contrast, it is clear that although the observed activity of calcined $\text{W}-\text{Zn}/\text{SnO}_2(\text{IMP})$ is still predominantly heterogeneous, a non-negative, hot-separation test was obtained, suggesting that at least some W leaches into solution, subsequently catalyzing the reaction and leading to a decreased metal content. It is important to add that although performed at the same substrate/metal ratio, unsupported bulk WO_3 is significantly less active than the SnO_2 -supported analogue. This clearly indicates that although bulk WO_3 is both active and heterogeneous, achieving a high dispersion and surface availability is critical to attain high levels of activity.

To probe this further, both monometallic analogues were subsequently tested for reusability (Figure 6). As expected from its non-negative hot filtration performance, the stability and reusability of the impregnated analogue is much poorer than the physical mixture, which contains exclusively WO_3 .

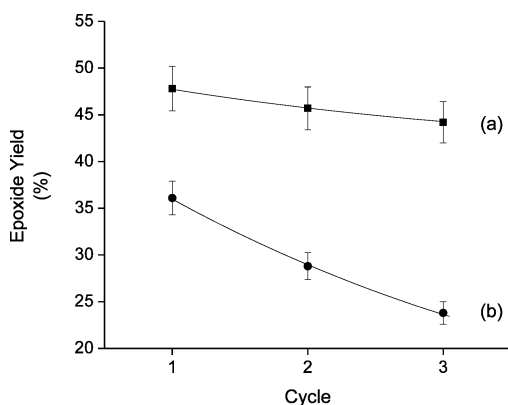


Figure 6. Recyclability of $\text{WO}_3/\text{SnO}_2(\text{PM})$ (a) and calcined $\text{W}/\text{SnO}_2(\text{IMP})$ (b). The catalyst was removed from the reaction solution, washed with 1-butanol, and dried overnight (16 h). Reaction conditions: cyclooctene in 1-butanol (1.0 M), olefin/ H_2O_2 molar ratio = 1.0, 80 °C, 4 h, 0.15 mol % W.

Specifically, the 30% decrease in activity by the third catalytic cycle suggests that impregnated W species possess rather poor stability on the solid support; along with leading to a background homogeneous reaction (and clouding judgment of the heterogeneous catalyst in the first cycle), this leads to a gradual loss in W content and the formation of much poorer catalyst. In contrast, within the experimental error, no decrease in performance was observed for $\text{WO}_3/\text{SnO}_2(\text{PM})$. This confirms that the mechanically mixed material is significantly more stable than the impregnated material and that WO_3 possesses greater stability than isolated tungstate species.

The Role of Zn. At this stage, it can be concluded that the most active and stable heterogeneous epoxidation phase is crystalline WO_3 and that mono- and polytungstate species, as formed initially on impregnated catalysts, are significantly more prone to leaching. Nevertheless, many questions remain unanswered. Why is $\text{W}-\text{Zn}/\text{SnO}_2$ more active than the monometallic analogue (per W^{VI} site) at a given set of pretreatment conditions? Why is the stability of the bimetallic system also so much higher than the analogous monometallic system? It seems that Zn is an essential constituent of the catalytic system, and its precise role deserves additional attention.

The first indication as to the crucial role of Zn was obtained from Raman analysis of the analogous samples, $\text{W}-\text{Zn}/\text{SnO}_2(\text{IMP})$ and $\text{W}/\text{SnO}_2(\text{IMP})$. Although both samples had been calcined under identical conditions (400 °C, 3 h), it is clear that when W is deposited onto the prefunctionalized support (Zn/SnO_2), a significantly larger amount of WO_3 is observed following pretreatment (Figure 7). Since WO_3 has

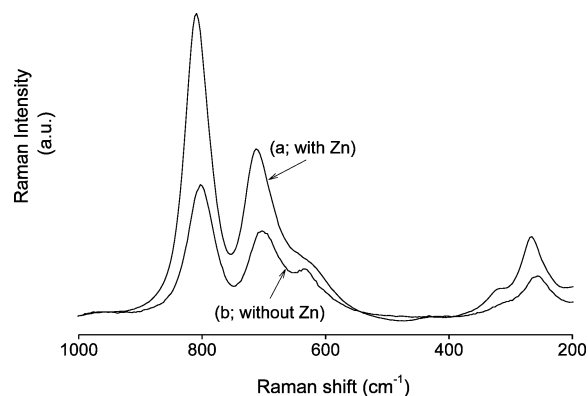


Figure 7. Raman spectra of $\text{W}-\text{Zn}/\text{SnO}_2(\text{IMP})$ (a) and $\text{W}/\text{SnO}_2(\text{IMP})$ (b) following calcinations at 400 °C for 3 h.

been shown to be the most active and stable epoxidation phase, it is clear that facilitating the transformation of mono- and polytungstate species into bulk WO_3 would account for both the increased activity per W^{VI} site and the stability of $\text{W}-\text{Zn}/\text{SnO}_2(\text{IMP})$. This would also account for the need to add the “dopant”, that is, Zn, onto the SnO_2 support prior to the deposition of W^{VI} .

To investigate further whether the role of Zn is to facilitate the phase change into WO_3 , the relative quantity of WO_3 present in $\text{W}-\text{Zn}/\text{SnO}_2$ was monitored for various amounts of Zn, keeping the W-loading constant. By taking the area of the 810 cm^{-1} WO_3 signal as 1.0 in monometallic $\text{W}/\text{SnO}_2(\text{IMP})$, the relative amount of WO_3 can be plotted against the total Zn content of the material. As can be seen (Figure 8), the addition of Zn onto the SnO_2 support prior to W deposition

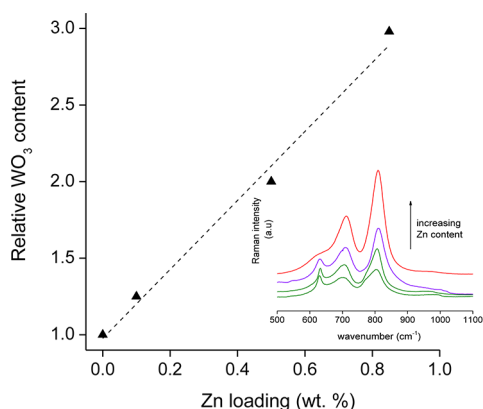


Figure 8. Relative WO_3 signal observed for $\text{W-Zn/SnO}_{2(\text{IMP})}$ at various Zn loadings. The total W content was equal for each material (3.5 wt %), and each sample was measured after calcination at $400\text{ }^\circ\text{C}$ for 3 h.

significantly facilitates the transformation of the as prepared mono- and polytungstate species into bulk WO_3 , the active and stable heterogeneous epoxidation phase.

The utilization of cationic dopants to facilitate phase changes is a frequent strategy in heterogeneous catalysis. For example, the doping of W/SiO_2 with Na leads to significant increases in catalytic activity for the oxidative coupling of methane.¹⁹ Palermo et al. reported that within the trimetallic Mn, Na, W formulation, Na plays a dual role, first facilitating a phase transition from methane-burning amorphous silica to crystalline and selective α -cristobalite.¹⁹ Furthermore, the addition of Na was found to lead to the stabilization of the catalytically active W phase, WO_4 , and consequently increase the activity and lifetime of the catalyst.¹⁹ Apparently, the role of Zn in the present system is to increase the mobility of the deposited mono- and polytungstate species such that the transformation to the active and stable epoxidation phase, WO_3 , can proceed efficiently during calcination.

Optimized Material Synthesis. From the experimental data discussed above, it becomes clear that the active species in this catalytic system is bulk WO_3 and that the role of Zn is to facilitate the transformation of the initial mono- and polytungstate species into the more active and stable oxide. Nevertheless, the reported catalytic system is prepared by a double impregnation procedure. Although impregnation procedures are commercially performed, a multistep procedure is both tedious and time-consuming. In addition, the requirement for two calcinations steps (at 300 and $400\text{ }^\circ\text{C}$) is energy-intensive and favors low dispersion of the catalytically active elements on the support surface.

Furthermore, although it has been demonstrated that by grinding bulk WO_3 and bulk SnO_2 together, similar catalytic activity can be obtained per W^{VI} site to the impregnated analogue, the unrefined nature of this, albeit rapid, technique leads to limitations in the form of poor dispersion and low W^{VI} surface availability. As such, alternative methods of preparation were considered, with the aim of obtaining highly dispersed WO_3 without support to increase the space time yield (STY), that is, the productivity per kilogram of catalyst. To this end, we aimed at the synthesis of nanosized WO_3 particles. Decreasing the particle size of WO_3 would, of course, lead to significant increases in available surface area and likely an increase in activity per W^{VI} site (i.e., turnover frequency, TOF).

Flame aerosol synthesis (herein, flame spray pyrolysis (FSP)) offers a convenient route to many (mixed) metal oxide heterogeneous catalysts.^{20,21} In particular, its ability to rapidly prepare high surface area materials with controlled properties in a continuous, single-step process is highly favorable on a large scale, as already shown as scales up to 1 kg/h .²² The procedure involves the pyrolysis of a continuous liquid feed containing appropriate metal precursors within a combustible solvent. In this way, the desired solid can be obtained in a single step, without need for high temperature calcination or multistage deposition.

As a proof of concept, pure WO_3 nanoparticles (npWO_3) were synthesized according to a previously reported procedure.¹⁶ X-ray diffraction (XRD) confirmed the nanoparticles consisted of WO_3 .²³ The specific surface area (SSA) determined by BET was $64\text{ m}^2/\text{g}$, corresponding to an average grain size of $\sim 13\text{ nm}$. Raman analysis of the obtained powder revealed that the particles were, indeed, crystalline WO_3 , and TEM analysis (Figure 9) confirmed the particle size measured

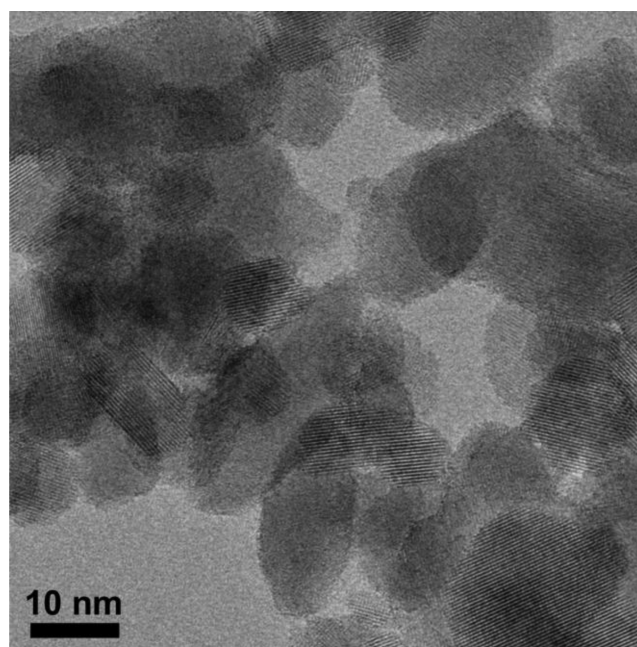


Figure 9. TEM image of npWO_3 powder.

by BET. As desired, the decrease in particle size leads to a significant increase in surface area, with the SSA of npWO_3 being ~ 11 times larger than that of $\text{W-Zn/SnO}_{2(\text{IMP})}$ (Table 2).

We subsequently evaluated the catalytic activity of npWO_3 against the impregnated reference catalyst, $\text{W-Zn/SnO}_{2(\text{IMP})}$. As can be seen (Table 2), a significant increase in activity per W^{VI} site is achieved with npWO_3 , with the TON and TOF increasing by 50% relative to the optimal impregnated material. Moreover, by removing the now-superfluous support material, the STY increases by 1 order of magnitude, from 2.3 to 81.7 h^{-1} . Similar to the $\text{WO}_3/\text{SnO}_{2(\text{PM})}$ material, the npWO_3 catalyst demonstrates a negative hot-filtration test, thus confirming the activity to be heterogeneous, and was found to be reusable (entry 2). We reason that this increase in activity (TON/TOF) is due to (i) the increased surface area (64 vs $6\text{ m}^2\text{ g}^{-1}$) of npWO_3 , (ii) the greater availability of WO_3 due to removal of the SnO_2 support, and (iii) the possibility that some residual,

Table 2. Catalytic Activity and Selectivity of Nanoparticulate WO₃ against Reported Reference Catalyst

entry	catalyst	procedure	S _(BET) m ² g ⁻¹	yield (%)	selectivity (%)	TON ^a	TOF ^b (h ⁻¹)	STY ^c
1	npWO ₃	FSP	64	84	>98	560	140	81.7
2	npWO ₃ 3rd use	FSP	60	86	95	573	143	83.6
3	W-Zn/SnO ₂	IMP	6	57	>98	380	95	2.3
4	WO ₃	commercial	8	21	>98	140	35	20.4

^aMole (epoxide formed) mole⁻¹ (W) h⁻¹. ^bMole (epoxide formed) mole⁻¹ (W) h⁻¹. ^ckg (epoxide formed) kg⁻¹ (cat) h⁻¹. Reaction conditions: cyclooctene in 1-butanol (1.0 M), olefin/H₂O₂ molar ratio = 1.0, 80 °C, 4 h, 0.15 mol % W.

isolated tungstate species remain in W-Zn/SnO₂, that is, that quantitative conversion of the as-deposited tungstate species into WO₃ is not observed. Indeed, the lower activity of commercial WO₃ clearly supports the important influence of surface area on catalytic activity (entry 4).

It is clear therefore, that by undertaking a detailed investigation of each constituent of the aforementioned catalytic system and by determining the true active species and the roles of the dopants that a significantly more active and productive catalyst has been prepared from a rationalized, scientifically justified basis. It should be stressed that STY is the benchmark evaluation of a heterogeneous catalyst, and that significant increases in STY have a profound impact on the scalability and feasibility of a heterogeneous catalyst on a large scale.⁵

CONCLUSIONS

Through a combination of catalytic and spectroscopic investigations, it has been demonstrated that the most active and stable species within W^{VI}-based epoxidation catalyst is bulk WO₃, and not mono- and polytungstate species as previously proposed. By determining this critical feature, more efficient preparation procedures lead to significant increases in both activity and productivity. Optimal catalytic activity was obtained over nanoparticulate WO₃ powder prepared by flame spray pyrolysis, which lead to a 50% increase in TON and TOF, and an order of magnitude increase in the observed space time yield.

EXPERIMENTAL SECTION

Catalyst Synthesis. W(-Zn)/SnO₂ was prepared according to the impregnation procedure reported by Kamata et al.¹⁵ WO₃/SnO₂(PM) samples were prepared by mechanically grinding the desired quantities of WO₃ and SnO₂ in a mortar and pestle for a total of 15 min. Where applicable, samples were calcined in air prior to use. Bulk WO₃ was obtained from Merck.

Nanoparticle Synthesis. A flame spray pyrolysis (FSP) reactor²³ was used for synthesis of WO₃ nanoparticles. A 0.2 M solution of ammonium (meta)tungstate hydrate (Aldrich, >97%) in diethylene glycol monobutyl ether/ethanol was supplied at a feed rate of 5 mL/min through the FSP nozzle and dispersed to a fine spray with 5 L/min of oxygen (Pan Gas, 99.5%) with a constant pressure drop of 1.5 bar at the nozzle outlet. The spray was ignited by an annular premixed methane/oxygen flame (CH₄ = 1.25 L/min and O₂ = 3.2 L/min) surrounding the nozzle. In addition, 5 L/min of oxygen was supplied by a surrounding porous ring to ensure over-stoichiometric and complete combustion. Particles were collected with a vacuum pump (Vacuumbrand, RE 16) on a water-cooled, glass-fiber filter (Albet, LabScience, 257 mm diameter) 50 cm above the burner.

Catalyst Characterization. X-ray diffraction patterns were obtained by a Bruker, AXS D8 Advance diffractometer operated at 40 kV, 40 mA at 2θ (Cu Kα) = 10–60°, step = 0.01°, and scan speed = 0.05°/s. The crystal size (d_{XRD}) was determined using the Rietveld fundamental parameter method with their structural parameters. The powder specific surface area was measured by BET analysis using a Micromeritics Tristar 3000. TEM analysis was performed on a Hitachi H600, operated at 100 kV. Raman analysis was performed on a Renishaw inVia microscope at 514 nm excitation.

Kinetic Evaluation. Catalytic evaluation was carried out in a 50 mL, three-necked, round-bottomed flask, equipped with a magnetic stirrer bar. The reactor was charged with the reactant solution (1 M cyclooctene in 1-butanol, or 0.2 M 1-hexene in dimethyl carbonate) and the desired amount of catalyst and stirred at reaction temperature (80 °C) for 15 min. Hydrogen peroxide was subsequently added to reach the desired alkene/oxidant ratio, and the reactions were performed for the desired length of time. Where appropriate, the solid catalyst was removed from the solution after a given period, with the activity of the filtrate monitored for an additional reaction period. All the reaction products were identified and quantified by GC/FID analysis (30 m FFAP column).

ASSOCIATED CONTENT

Supporting Information

Additional experimental details and results. This material is available free of charge via the Internet at <http://pubs.acs.org>.

AUTHOR INFORMATION

Corresponding Author

*E-mail: ive.hermans@chem.ethz.ch.

Notes

The authors declare no competing financial interest.

REFERENCES

- Rebsdat, S.; Mayer, D. In *Ullmann's Encyclopedia of Industrial Chemistry*; Wiley: Weinheim, 2001, p 547.
- Sheldon, R. A. *Chem. Commun.* **2008**, 3352.
- Venturello, C.; Dalosio, R.; Bart, J. C. J.; Ricci, M. J. *Mol. Catal.* **1985**, *32*, 107.
- Ishii, Y.; Yamawaki, K.; Ura, T.; Yamada, H.; Yoshida, T.; Ogawa, M. *J. Org. Chem.* **1988**, *53*, 3587.
- Cavani, F.; Teles, J. H. *ChemSusChem* **2009**, *2*, 508.
- Roman-Leshkov, Y.; Davis, M. E. *ACS Catal.* **2011**, *1*, 1566.
- Wu, P.; Tatsumi, T.; Komatsu, T.; Yashima, T. *J. Catal.* **2001**, *202*, 245.
- Blasco, T.; Cambor, M. A.; Corma, A.; Esteve, P.; Guil, J. M.; Martinez, A.; Perdigon-Melon, J. A.; Valencia, S. J. *Phys. Chem. B* **1998**, *102*, 75.
- Neumann, R.; Gara, M. J. *Am. Chem. Soc.* **1995**, *117*, 5066.
- Levecque, P.; Poelman, H.; Jacobs, P.; De Vos, D.; Sels, B. *Phys. Chem. Chem. Phys.* **2009**, *11*, 2964.

- (11) Hoegaerts, D.; Sels, B. F.; de Vos, D. E.; Verpoort, F.; Jacobs, P. A. *Catal. Today* **2000**, *60*, 209.
- (12) Kamata, K.; Yonehara, K.; Sumida, Y.; Yamaguchi, K.; Hikichi, S.; Mizuno, N. *Science* **2003**, *300*, 964.
- (13) Arends, I.; Sheldon, R. A. *Appl. Catal. A* **2001**, *212*, 175.
- (14) Bera, R.; Koner, S. *Inorg. Chim. Acta* **2012**, *384*, 233.
- (15) Kamata, K.; Yonehara, K.; Sumida, Y.; Hirata, K.; Nojima, S.; Mizuno, N. *Angew. Chem., Int. Ed.* **2011**, *50*, 12062.
- (16) Righettoni, M.; Tricoli, A.; Pratsinis, S. E. *Anal. Chem.* **2010**, *82*, 3581.
- (17) Bordiga, S.; Bonino, F.; Damin, A.; Lamberti, C. *Phys. Chem. Chem. Phys.* **2007**, *9*, 4854.
- (18) Corma, A.; Nemeth, L. T.; Renz, M.; Valencia, S. *Nature* **2001**, *412*, 423.
- (19) Palermo, A.; Vazquez, J. P. H.; Lee, A. F.; Tikhov, M. S.; Lambert, R. M. J. *Catal.* **1998**, *177*, 259.
- (20) Schimmoeller, B.; Pratsinis, S. E.; Baiker, A. *ChemCatChem* **2011**, *3*, 1234.
- (21) Mädler, L.; Kammler, H. K.; Mueller, R.; Pratsinis, S. E. *J. Aerosol Sci.* **2002**, *33*, 369.
- (22) Mueller, R.; Maedler, L.; Pratsinis, S. E. *Chem. Eng. Sci.* **2003**, *58*, 1969.
- (23) Righettoni, M.; Tricoli, A.; Pratsinis, S. E. *Chem. Mater.* **2010**, *22*, 3152.